Kneading and Molding of Ceramic Microparts by Precision Powder Injection Molding (PIM)

S. Y. Yang,[1] C. K. Huang,[2] B. C. Lin,[1] W. C. J. Wei[3]

[1]*Department of Mechanical Engineering, National Taiwan University, Taiwan, Republic of China*
[2]*Department of Mechanical Engineering, Lunghwa University of Science and Technology, Kueishan, Taoyuan, Taiwan, Republic of China*
[3]*Institute of Materials Science and Engineering, National Taiwan University, Taiwan, Republic of China*

Received 7 April 2005; accepted 20 August 2005
DOI 10.1002/app.23010
Published online 10 January 2006 in Wiley InterScience (www.interscience.wiley.com).

ABSTRACT: This paper investigates the kneading and formability of microparts made using alumina in micropowder injection molding. In this study, quality feedstock with uniform powder dispersion was achieved when optimum kneading process was performed. In addition, the thin microplates were successfully manufactured using a custom-made injection machine. Shrinkage was significantly reduced in microspecimens when the mold temperature was increased to 70°C. The results of flow visualization were conformed to that of experiments in this study. A very important result for flow visualization and experiment was molten polymer filled the cavity by shortest period producing a least shrinkage in microparts. © 2006 Wiley Periodicals, Inc. J Appl Polym Sci 100: 892–899, 2006

Key words: blending; dispersions; injection molding; microstructure; plastics

INTRODUCTION

Ceramic injection molding (CIM) is a technique combining the injection molding (IM) of plastics and the processing of ceramic powders,[1,2] and offers the advantages of the fabrication of near-net-shape ceramic pieces with fairly complex configurations. The CIM technique has proven that the machining costs for the parts made using very hard materials are greatly cut down. For these reasons, the technique has gained the attention of the ceramic industry in the past decade.

Most microparts,[3] such as gears and fans, must possess high strength and wear resistance and have precise dimensions. However, plastic material alone cannot satisfy these requirements. Thus, the parts made by ceramics with excellent strength and good wear resistance are the best choice.

The difference between powder injection molding (PIM) and other forming techniques is the polymeric carrier, of which the free volume supplies a feedstock with flowing ability for IM. The particles will contact together after the binder removal. These changes affect the particle packing before sintering.[4,5] The defects, e.g., agglomeration, are still existing even after binder-burn-out and sintering. The mechanical properties of sintered parts will thus be decreased.[6]

Correspondence to: C. K. Huang (ckhunag@mail.me.lhu.edu.tw).

Journal of Applied Polymer Science, Vol. 100, 892–899 (2006)

The objective of kneading is to achieve uniform mixing, which leads to a good quality part. Song and Evans[7] showed their control in kneading process to manufacture various zirconia feedstocks. The powder agglomeration of the feedstock was held due to insufficient shear stress provided by the kneader. In this case, the agglomeration still existed after parts were sintered. Wu and Wei[8–10] conducted the measurements on torque–time–temperature (TTT) variation as a function of the temperature and the kneading speed. The agglomerated powders were shear-kneaded and uniformly dispersed in the binder. These results strongly revealed the ceramic feedstocks have a good quality only if the kneading process is conducted well.

The filling of the molten feedstock in small channel always accompany a high flow resistance. If the machine and mold are not properly designed and performed, the molten feedstock will instantaneously be jammed and consequently frozen in a tiny runner or cavity, resulting in a short-shot and apparent warpage.[11] Higher injection rates are needed especially for a highly thermoconductive ceramic feedstock to achieve a shorter heat-transferring period, to offer a greater shear-thinning effect. Fast injection is helpful to maintain the molten flow behaving at low viscosity.[12,13] The formability of the microparts must be closely controlled by the injection rate and the IM machine.

This research first developed the optimum kneading process for alumina powder/binder system to achieve a uniform quality. The other purpose of this study was to understand the formability of mi-

TABLE I
Properties of Al_2O_3 Powders

BET (m^2/g)	9.0
Specific gravity	3.97
Particle size (μm)	0.4
Crystalline phase	α
Purity (%)	99.7
Impurity	Na_2O (800 ppm), SiO_2 (800 ppm), Fe_2O_3 (100 ppm), MgO (500 ppm)

crospecimens, using a custom-made injection machine. Flow visualization was an effective method and was established in this study to observe and understand the flow-related phenomena.

EXPERIMENTAL

Materials and specimens

The raw materials used in this study include alumina powder, polypropylene, paraffin wax, and stearic acid. The aluminum powder, A-16SG, was supplied by Alcoa Industrial Chemicals (USA). Polypropylene (PP; Formosa Plastic, Taiwan) and paraffin wax (PW; Nippon Serio, Japan) were used as a binder and dispersive medium, respectively, in the formulation to provide fluidity. Stearic acid (SA; Nacalai Tesque, Japan) acted as a surfactant for the alumina and polymeric ingredients, and effective as a dispersant. The properties of four materials are listed in Tables I and II. The constitution of the additives, using the best formulation, has been reported earlier.[14] The constitution of polymer additives is in a weight ratio of PW: PP:SA = 70:25:5 and the mass ratio of alumina to plastic ingredients is 85:15, which is equivalent to a volume of 56.6 to 43.4, for the overall constitution. Thin specimens with dog-bone shape, according to ASTM D638, as shown in Figure 1, with 12 mm in length, 2.5 mm in width, 0.2 mm and 0.15 mm, respectively, in thickness, were prepared.

Kneading and granulation

A twin Σ-type kneader (Ray-E Manufacture Co., Tainan, Taiwan) with a mixing bowl of 0.65 L was used and operated at a rate of 30 rpm. In the beginning of the kneading process, alumina powder was preheated to 200°C in the kneader. Three chemical ingredients were then mixed with the powder in a sequence as indicated. PP was first added to form a mixture. After mixing for 20 min, SA was then added and the temperature of the kneader was reduced to 180°C. Twenty minutes later, PW was gradually put in the bowl, as the temperature of the mixture reached 150°C. Each constituent was mixed well with the alumina in the kneader for additional 20 min. The dough-type mixture was then gradually granulated as the temperature of the bowl decreased to 70°C. One kneading and granulation process took approximately 150 min.

Custom-made IM machine and processing

The parts tested in this study are formed using a custom-made IM machine, as shown in Figure 2, which has many functions making it suitable for various IM operations. The machine mainly includes clamping, melting, and injection units. The movable and fixing plates are fixed on the clamping device. Therefore, it can move forward and backward under pressure exerted by rotating a hand-wheel on the device. The mold is locked in a fixing plate, using bolts. The melt unit mainly uses a hot runner to provide melting energy for feedstock. Inside the hot runner, there is an injection sleeve with a 2-mm diameter hole, which serves as the barrel of the machine. The injection unit mainly includes one injection plunger and an air cylinder. A vacuum pump is attached to remove air or emissive gas during mold filling.[15]

The image capture system is illustrated in Figure 3. The system utilizes a reflection mirror inserted in the mold to reflect the cavity image, and uses a high-speed video camera (KODAK Motion Corder Analyzer) to record the mold-filling images at a rate of 1000 films/s in the injection interval.

In this experiment, the air pressure and the molding temperature are two significant processing parameters. In comparison, melt temperature is not a sensitive parameter in the production of small parts.[16] Thus, we kept the melt temperature at a constant value, 150°C, to find the processing window of previous two parameters. Short-shot or flash in the IM parts was indicated outside the boundary of the processing window. The permissible injection pressure, called mechanical ability, cannot exceed 8 kgf/cm^2 in this window.

Debinding and sintering

An organic solvent *n*-heptane (total isomers is more than 9.8%, water content ≤0.01%, free acid ≤0.01%) was used to extract PW and SA in the specimens. The solvent debinding was conducted at 60°C and held for 2.5 h. After drying, the specimens were subjected to thermal debinding, according to the conditions indi-

TABLE II
Properties of Polymeric Materials

Polymeric Ingredients	T_m (°C)	Specific Gravity
Paraffin wax (PW)	68	0.918
Polypropylene (PP)	170	0.903
Stearic acid (SA)	71.9	0.978

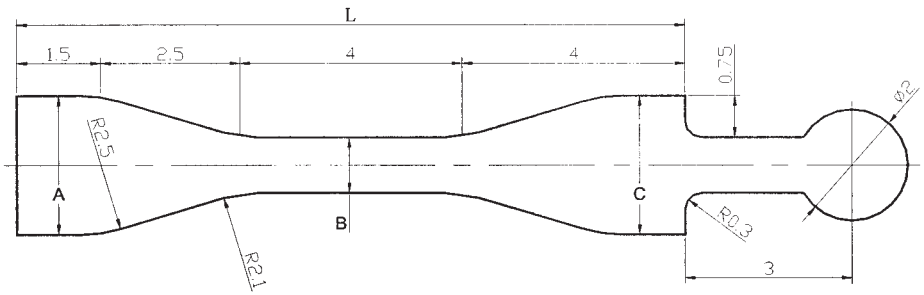

Figure 1 The geometry and dimensions of thin microspecimen.

cated in Table III. The specimens after debinding were checked to ensure that the surfaces were free from any visual defects, e.g., flaws. The samples were then heated at a rate of 10°C to the sintering temperature of 1580°C, and were maintained at that temperature for 1 h.

Quality evaluation

To examine the shrinkage and formability of parts, thin microspecimens with a 0.20-mm thickness were tested in this study. They were measured with a coordinate measurement machine (CMM; Poly, Italy). The precision level of the measurements was 1 μm. The shrinkage (η) could be calculated in terms of the average length (d) of green parts and average length (d') of sintered parts as follows:

$$\eta = \frac{d - d'}{d} \times 100\% \quad (1)$$

The denoted length d is the widths A, B, C, and length L, respectively, in thin microspecimen, as shown in Figure 1. The average shrinkage was determined based on six specimens for every tested sample.

RESULTS AND DISCUSSION

Kneading response of feedstock

The kneading response of the alumina feedstocks was measured by the torque rheometer, as shown in Figure 4. The torque profile shows an increase of the torque value over the first few minutes, because the PP changes from a solid state to a molten state while mixing with the powder. The first peak is so called "loading peak," the powder and PP binder are mixed to produce a granular state. The second peak is called the fusion peak, the binder is heated and coated on the powder to get a dough state. The feedstock is then in dough stage in 20 min and produces consistent properties in another 20 min after surfactant SA is added to polymer compound. In other words, the homoge-

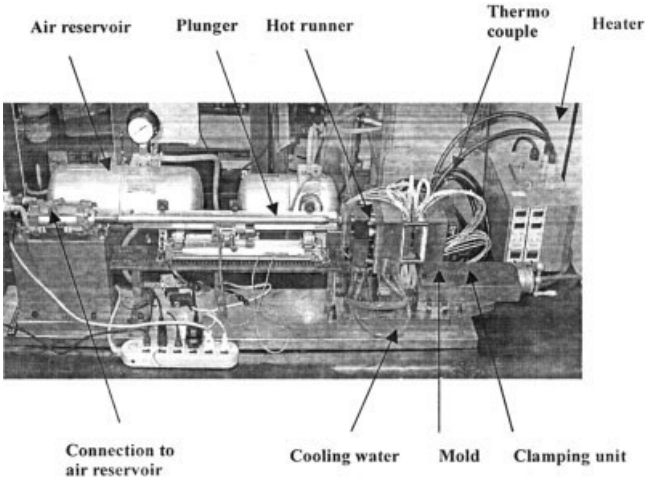

Figure 2 Custom-made microinjection machine.

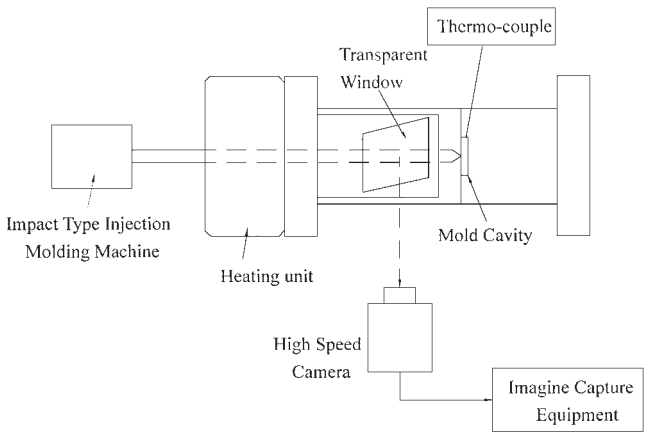

Figure 3 Schematic diagram showing the setup of image captures system.

TABLE III
Stages of the Thermal Debinding for Al_2O_3 Microparts

Stage	Ramping Rate (°C/min)	Isothermal Temp. (°C)	Holding Time (h)
1	2	200	0.3
2	2	260	2
3	5	400	0
4	10	1000	0.5
5	Furnace cooling	—	—

neous feedstock is produced when the powders are uniformly dispersed in the polymer compound.

Figure 5 shows the microstructures of two feedstocks observed by transmission optical microscope (OM). In Figure 5(a), the black features in dough stage were the powder agglomerates in the feedstock, by the kneading conditions of 180°C/30 rpm after the SA surfactant was added into the mixture for 3 min. The homogeneity of the feedstock was poor. However, the dough kneaded at 150°C/30 rpm for 20 min had great improvement on the homogeneity, as shown in Figure 5(b). In other words, the powders were uniformly dispersed in the polymeric compound when surfactant is added and kneaded with enough time. The results also revealed that SA was a good dispersive agent for alumina feedstock. In this experiment, the made feedstock was used to fabricate thin microspecimens as described later.

SEM (scanning electron microscopy, Japan JSM-6500F) micrograph of the polished and thermally etched surface of a sintered part is shown in Figure 6.

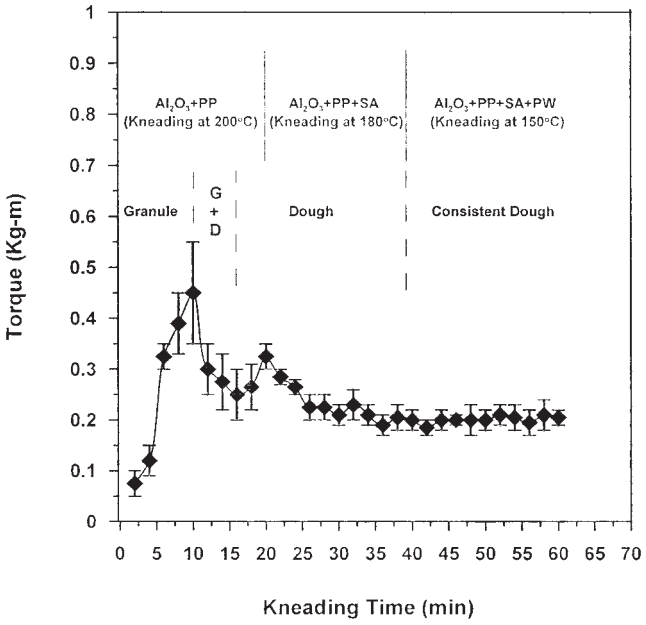

Figure 4 Kneading torque–time profile of an alumina feedstock.

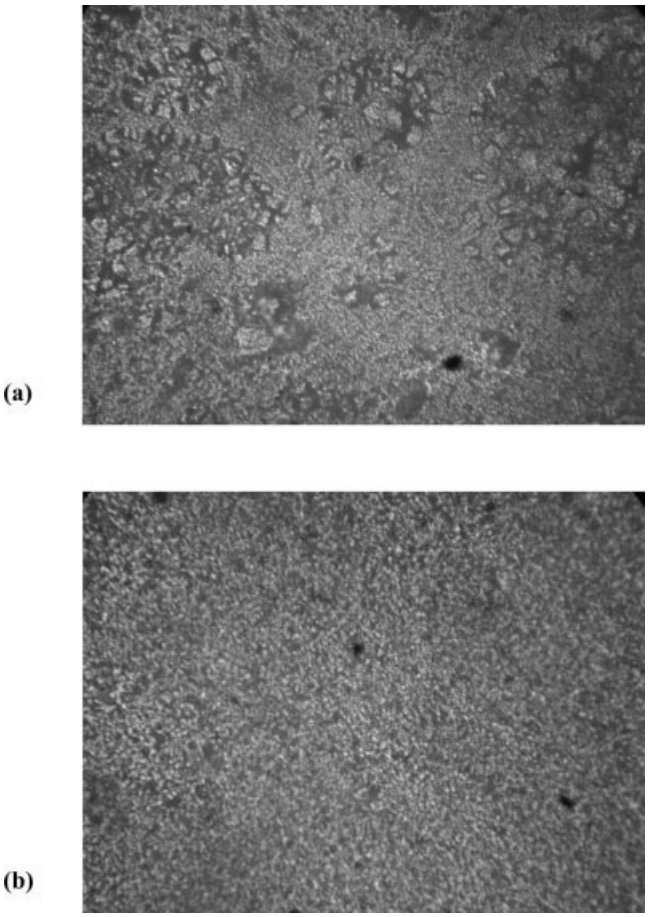

Figure 5 Transmission OM images (magnification 500×) of thin feedstocks kneaded after the SA surfactant was added into the mixture for (a) 3 min and (b) 20 min.

The microstructure of the sintered Al_2O_3 shows uniform grain structure in a dense matrix. It confirms that the kneading process with SA additive used in this study is appropriate.

Processing window for microspecimens

The processing window of the microspecimens is shown in Figure 7. Short-shot is produced in parts

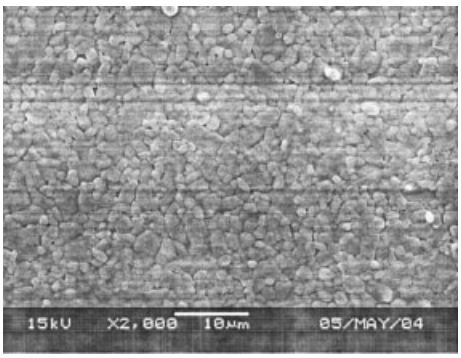

Figure 6 SEM image of the homogeneous ceramic specimen after sintering at 1580°C for 1 h.

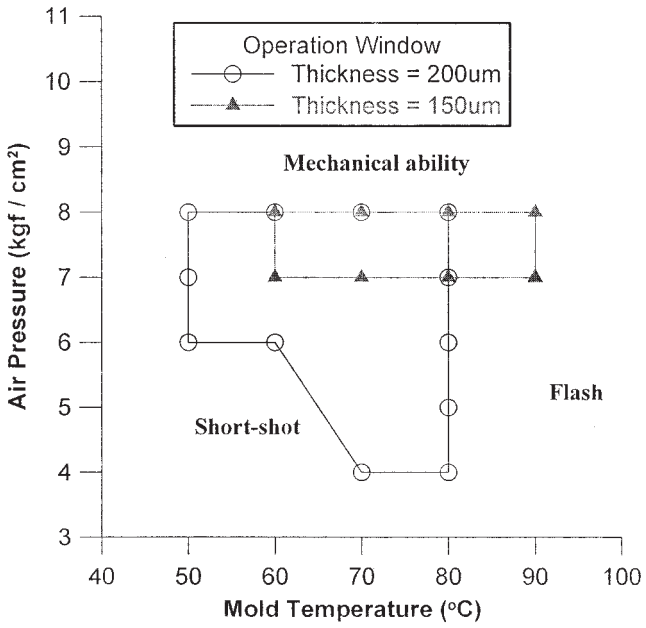

Figure 7 Processing window of thin microspecimens.

when processing exceeds the left-hand boundary of the window. Flash occurs in parts when processing exceeds the right-hand boundary of the window. In addition, the mechanical ability of the injection machine is exceeded when processing exceeds the top boundary of the window. The formability of the ceramic feedstock is favorable when the processing window is larger. The quality of microspecimens is not acceptable when the processing parameters are out of the range of the window.

The processing zone of micro specimen with a thickness of 0.2 mm is significantly larger than that of 0.15 mm. A frozen layer formed as the molten polymer flowed into the thinner cavity. In other words, a higher pressure was needed to drive the molten feedstock to fill the cavity before it froze. Thus, in thin micropart molding, a high pressure and a high mold temperature were necessary to produce high-quality parts.

One photograph of the green microspecimen with a thickness of 0.2 mm is shown in Figure 8. The average mass of the part is 13.6 mg. From the photograph it appears that the thin micropart was well formed with clear structural definition. However, serious deflection (warpage) of some specimens, when molding at 70°C and an air pressures of 4 kgf/cm^2, occurred after sintering, as shown in Figure 9. The nonhomogeneity (e.g., residual stress) might exist in the warping specimens, when the injection pressure was lower. Lower injection pressure did not carry out symmetric molding filling, and the residual stress of the specimens could not be released in debindng and sintering stages.

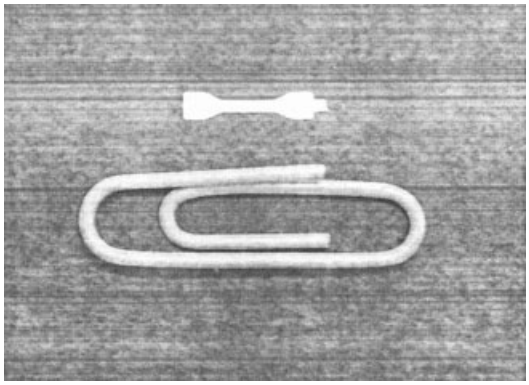

Figure 8 A photograph of the green part with a thickness of 0.20 mm, comparing to a clip.

Shrinkages in microspecimens

The linear shrinkage results with small error deviations of the sintered microceramic specimens with a thickness of 0.20 mm are shown in Figure 10, which indicates significant decrease in the shrinkage as the mold temperature is set at 70°C. When the mold temperature was kept lower than the glass-transition temperature (T_g), a frozen layer is readily formed as the molten feedstock flows into the cavities. However, a flash of the injection occurred in the specimens when the mold temperature reached 80°C.

In addition, the width B had the largest shrinkage and the length L had the smallest shrinkage when the mold temperatures were less than 70°C. Molten polymer easily formed a frozen layer, retarding the filling of molten polymer in necking area. Thus, a higher shrinkage occurred in the neck width after the parts were sintered. To further understand the reasons, the specimen with a thinner thickness of 0.15 mm was tested to illustrate its formability by various mold temperatures. Figure 11 shows the flowing length of the ceramic parts with a thickness of 0.15 mm increases when the mold temperature was increased. Shot-shot occurred in the microspecimen as the mold

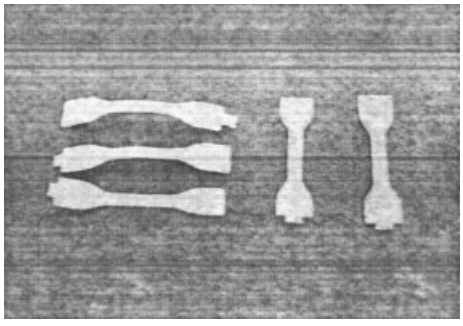

Figure 9 A photograph illustrating the deflection occurred in the sintered ceramic specimens when a lower injection pressure was used.

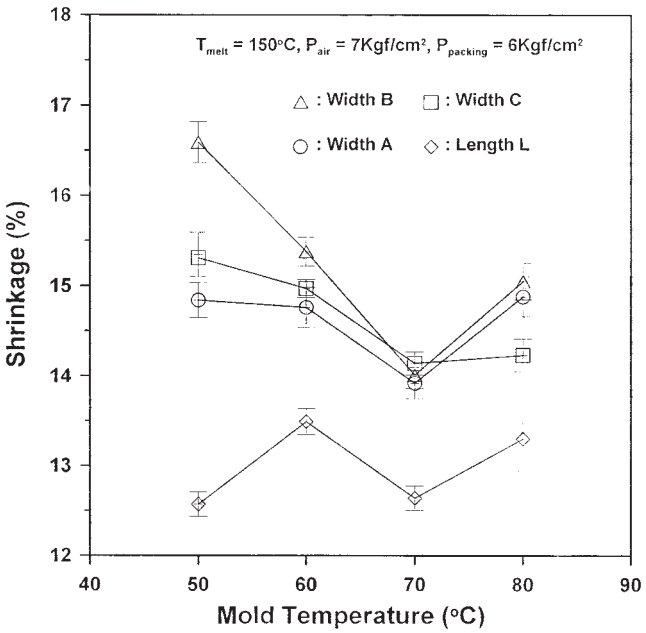

Figure 10 Sintering shrinkage of the ceramic specimens prepared by various mold temperatures.

temperature was less than 80°C. However, the short-shot occurred in a microspecimen with a thickness of 0.20 mm at a lower mold temperature of 50°C. This clearly revealed a thinner part needed higher mold temperature to increase the formability. That is, thin and narrow specimens can be duplicated well with increasing the mold temperature.

Flow visualization

Figure 12 displays the images of melt flow in glass mold with a cavity of 12 × 2.5 × 0.2 mm^3 during filling process. It was found that the melt front advanced over the cavity in a short period and completely filled in 5.5 ms. The filling flow in cavity could be divided into two stages. One was rapid-flowing stage, and the other was stable-flowing region. The rapid filling stage took place at the instant of the impact of the hammer on the plunger. The subsequent stable-filling stage proceeded as the plunger was thrust until the cavity was filled completely. Thus, the increase of the impact energy shall broaden the rapid-flowing stage.

Figure 13 shows the melt front during the filling process in the cavities at different mold temperatures. It shows that the mold temperature is the dominant parameter of impact type micro-IM. The increase in the mold temperature significantly reduced the filling time, reducing from 5.5 to 3.0 ms, as the mold temperature is increased from 50°C to 70°C. However, the filling time was 3.5 ms when the mold temperature was kept at 80°C. It is easy to understand that the mold temperature determines the amount of heat flux and preserve melt at higher temperature during the injection stage. It is helpful to fill the cavity at a lower viscosity that will increase the filling speed. Therefore, the decrease of part width or thickness would indicate the importance of mold temperature.

The filling time was the shortest and the shrinkage was the least when the specimens were injected at the mold temperature of 70°C. The contrary case was molding at 50°C. That is, molten polymer filled the cavity by shortest period produced a least shrinkage. The mold filling results are consistent to the flow visualization analysis.

CONCLUSIONS

Based on this study on the kneading and formability of ceramic material in the micro-IM, the following conclusions can be drawn.

1. The torque–time profile of kneading alumina feedstock was reported by using a twin screw kneader. The homogeneity of the feedstock gradually improved after the SA surfactant was added into the mixture. The microstructure of the sintered specimens was uniform and dense due to the homogeneity of the feedstock.
2. Microspecimens were successfully manufactured using a custom-made injection machine, when a high mold temperature and an appropriate air pressure were used within the operation window.
3. Sintering shrinkage was significantly reduced when the mold temperature increased to 70°C. A larger shrinkage occurred in the thin and narrow dimensions because a frozen layer was easily formed in the region. On the contrary, the smaller shrinkage occurred in thick dimensions because the molten polymer was easily filled in the cavity.
4. The results of flow visualization displayed the flow situation in the cavity, and could be divided into two stages. The rapid-flowing stage occurred at hammer impact, and the stable-flowing stage

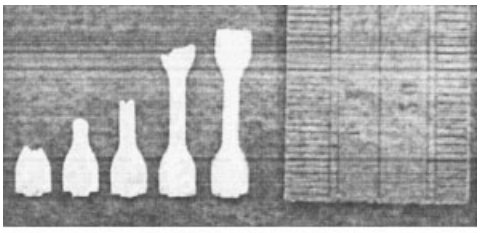

Figure 11 Formability tests for thin microspecimens with a thickness of 0.15 mm, by various mold temperatures.

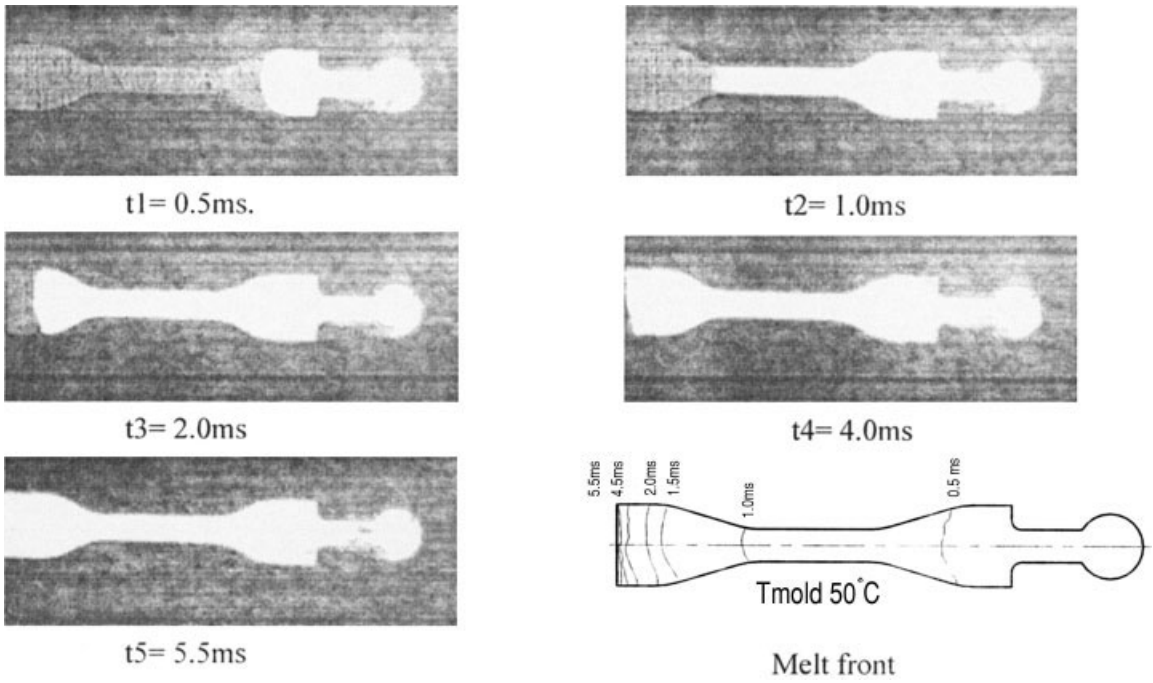

Figure 12 The images of melt flow in a glass mold with a thickness of 0.2 mm during filling test at a melt temperature of 150°C, an air pressure of 7 kgf/cm^2, a packing pressure of 6 kgf/cm^2, and a mold temperature of 50°C.

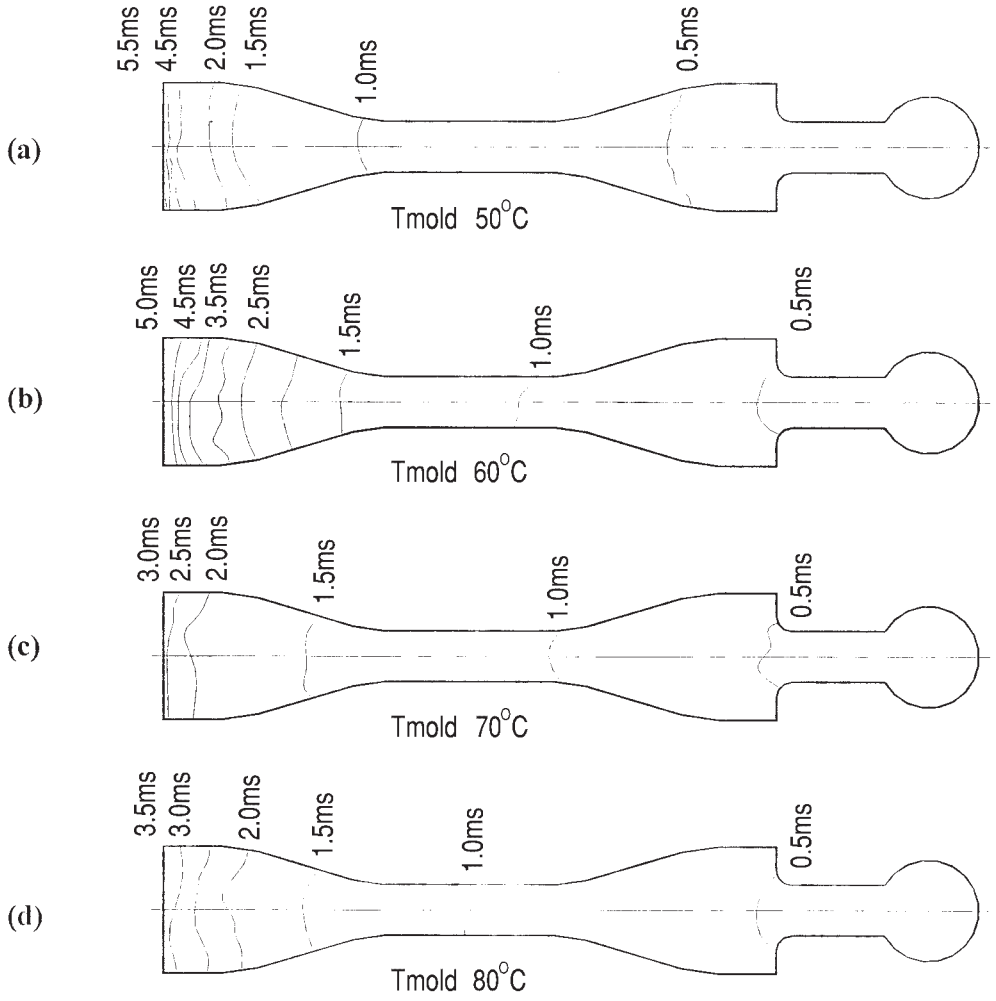

Figure 13 The location of melt fronts during the filling process conducted at a melt temperature of 150°C, an air pressure of 7 kgf/cm^2, a packing pressure of 6 kgf/cm^2, and the mold temperatures of (a) 50°C, (b) 60°C, (c) 70°C, and (d) 80°C.

took place by a continuous filling. Higher mold temperature enabled the melt with a reduced viscosity to fill the cavity easily. The molten polymer filled the cavity by shortest period produced a least shrinkage. The mold filling results are consistent to the flow visualization analysis.

References

1. German, R. M. Powder Injection Molding; MPIF: Princeton, NJ, 1990.
2. Mutsuddy, B. C.; Ford, R. G. Ceramic Injection Molding; Chapman and Hill: London, 1995.
3. Kukla, C.; Loibl, H.; Detter, H. Kunststoffe Plast Europe 1998, Sept., 1331.
4. Wright, J. K.; Edirisinghe, M. J.; Zhang, J. G.; Evans, J. R. G. J Am Ceram Soc 1990, 73, 2653.
5. Zhang, J. G.; Edirisinghe, M. J.; Evans, J. R. G. J Eur Ceram Soc 1989, 5, 63.
6. Hunt, K. N.; Evans, J. R. G.; Woodthrope, J. Br Ceram Trans J 1998, 87, 17.
7. Song, J. H.; Evans, J. R. G. J Mater Sci Lett 1994, 13, 1642.
8. Wu, R. Y.; Wei, W. C. J. J Eur Ceram Soc 2004, 24, 3653.
9. Wu, R. Y.; Wei, W. C. J. Ceram Process Res 2004, 5, 274.
10. Wu, R. Y.; Wei, W. C. J. J Eur Ceram Soc 2005, 88, 1734.
11. Despa, M. S.; Kelly K. W.; Collier, J. R. Microsystem Technologies, 6, pp. 60–66, (1999).
12. Fasset, J. Plast Eng 1995, Dec., 35.
13. Kleinebrahm, M. Kunststoffe Plast Europe, 1998, Jan, 41.
14. Wei, W. C. J.; Wu, R. Y.; Ho, S. J. J Eur Ceram Soc 2000, 20, 1301.
15. Yang, S. Y.; Nian, S. C.; Sun, I. C. Int Polym Process 2002, 17, 355.
16. Eberle, H. Kunststoff Plastic Europe, 1998, Sep, 1344.